Stoyan Nedeltchev[1]
Swapna Rabha[1]
Uwe Hampel[1,2]
Markus Schubert[1]

[1]Helmholtz-Zentrum Dresden-Rossendorf, Dresden, Germany.

[2]AREVA Endowed Chair of Imaging Technologies in Energy and Process Engineering, Dresden University of Technology, Dresden, Germany.

A New Statistical Parameter for Identifying the Main Transition Velocities in Bubble Columns*

The identification of the main flow regime boundaries in bubble columns is essential since the degrees of mixing and mass and heat transfer vary with the flow regime. In this work, a new statistical parameter was extracted from the time series of the cross-sectional averaged gas holdup. The measurements were performed in bubble columns by means of conductivity wire-mesh sensors at very high sampling frequency. The columns were operated with an air/deionized water system under ambient conditions. As a flow regime indicator, a new dimensionless statistical parameter called "relative maximum number of visits in a region" was introduced. This new parameter is a function of the difference between the maximum numbers of visits in a region, calculated from two different division schemes of the signal range.

Keywords: Bubble columns, Conductivity wire-mesh sensor, Flow regime identification, Gas holdup, Hydrodynamics

Received: November 30, 2014; *revised:* September 17, 2015; *accepted:* September 18, 2015

DOI: 10.1002/ceat.201400728

1 Introduction

Bubble columns find broad application as reactors and separation units in the chemical, mining, pharmaceutical, and biochemical industries. These gas-liquid contactors consist of a discontinuous gas phase (in the form of bubbles) moving relative to a continuous phase (a liquid or slurry). They can be single-staged or multi-staged, liquid-batch or continuous, operated co-currently or counter-currently. Bubble columns have a wide range of applications such as absorption, stripping, catalytic slurry reactions (such as Fischer-Tropsch synthesis), bioreactions, coal liquefaction, fermentation, etc. Comprehensive information about bubble columns and their applications is available in [1]. In bubble columns, the rate of transport of the gas phase to the liquid phase often limits the productivity and is therefore a critical design criterion. The uncertainty in today's bubble column design arises from a lack of fundamental understanding of their complex flow characteristics.

Bubble dynamics and hydrodynamic regimes indirectly influence the scale-up and design of bubble column reactors. The main transition velocities U_{trans}[1)] are important design parameters for bubble columns. A thorough knowledge of these parameters is necessary for a proper scale-up of bubble columns. In particular, the degree of mixing and the heat and mass transfer – and thus, the whole bubble column performance (especially the achievable conversion) – depend on the prevailing flow regime. Therefore, it is important to identify and to be able to predict the conditions under which the transition from bubbly flow to the churn-turbulent flow regime occurs. An example of the effect of the prevailing flow regime on the hydrodynamic parameters can be drawn from the gas holdup correlations. In general, the exponent of U_G varies from 0.7 to 1.2 in the gas holdup correlations recommended for the bubbly flow regime, whereas in the churn-turbulent flow regime the effect of U_G is less pronounced and correlations reveal exponent values of 0.4–0.7. In addition, the first U_{trans} value (distinguishing the end of the bubbly flow regime and the onset of the transition regime) plays an important role in the calculation of the equilibrium (large) bubble size and the large bubble holdup, which determine the mass transfer rates [2]. So, the development of a reliable method for its identification is essential.

Only for aqueous liquid systems such as water, electrolyte solutions, etc., approximate flow regime maps (for instance, presented in [1]) are currently available. These steady empirical flow regime maps predict a certain flow pattern for given volume flow rates of liquid and gas. However, they are neither able to predict the change of the flow pattern along the flow path (in case of stationary flows) nor the time- and space-dependent flow structure (in case of transient flows). For the design and

Correspondence: Dr. Stoyan Nedeltchev (snn13@gmx.net), Dr. Markus Schubert (m.schubert@hzdr.de), Helmholtz-Zentrum Dresden-Rossendorf, Bautzner Landstrasse 400, 01328 Dresden, Germany.

*S. Nedeltchev, M. Schubert, T. Donath, S. Rabha, U. Hampel, *2nd Int. Symp. on Multiscale Multiphase Process Engineering (MMPE-2)*, Hamburg, September **2014**.

1) List of symbols at the end of the paper.

scale-up of bubble columns, the effects of the fluid properties and the nature of the gas distributor on the flow regime boundaries require detailed examination.

1.1 Main Flow Regimes in Bubble Columns

In bubble column reactors, the hydrodynamics, transport and mixing properties such as pressure drop, holdups of various phases, fluid-fluid interfacial areas, and interphase mass and heat transfer coefficients depend strongly on the prevailing flow regime. The gas-liquid flow pattern is affected by the bubble formation and coalescence rates. As the superficial gas velocity U_G increases, three different flow regimes are being formed:

- *Bubbly flow (homogeneous) regime*: This regime is characterized by relatively small and rather uniform bubbles with equal radial bubble and gas holdup distributions. There is a gentle agitation of the gas-liquid dispersion and insignificant bubble coalescence.
- *Transition flow regime*: This regime is characterized by a widened bubble size distribution and local liquid circulation patterns. It is formed because the transition from bubbly flow to the churn-turbulent flow regime is a gradual process.
- *Churn-turbulent (heterogeneous) regime*: At U_G values higher than 0.05 m s^{-1}, the homogeneous gas-liquid dispersion cannot be maintained and an unsteady flow pattern (with channeling) occurs. The churn-turbulent flow regime is characterized by large bubbles (formed due to coalescence) moving with high rise velocities ($\geq$ 0.8 m s^{-1}) in the presence of small bubbles [3]. The large bubbles take the form of spherical caps with a very mobile and flexible interface. These large bubbles can grow up to a diameter of about 0.15 m [1]. The churn-turbulent flow regime is most commonly encountered in industrial bubble columns [4]. It is characterized by the establishment of gross circulation patterns, the existence of a pronounced radial gas holdup profile, and vigorous mixing. The transition from bubbly flow to the churn-turbulent flow regime is usually accompanied by a sharp increase in the interstitial gas velocity (the mean rise velocity of the bubbles in a bubble swarm).

It is noteworthy that Franz et al. [5] described the flow in a bubble column as a wide distribution of vortices following in a stochastic sequence. The authors divided the gas-liquid dispersion into three zones: A region of homogeneous turbulence (swarm turbulence) exists in the core of the column and bubble coalescence prevails especially at high U_G values; in the annulus of the column, a relatively bubble-free zone exists and the flow there occurs in downward direction; between these two regions there is a zone with a high velocity gradient and free anisotropic turbulence and most of the re-dispersion of the gas phase takes place there. Franz et al. [5] also confirmed the existence of a stable axially asymmetric flow structure in the bubble column.

1.2 Previous Methods for Flow Regime Identification

Different methods for the differentiation of the boundaries of the main flow regimes in bubble columns have been proposed in the literature. The most important ones are summarized in Tab. 1. They are all well-known and standard methods.

In addition, Bhole and Joshi [18] used the theory of linear stability in order to identify the main transition velocity. It has been also demonstrated that computational fluid dynamics (CFD) simulations [19–21] are capable of identifying the main transition velocities. Olmos et al. [22] applied different techniques (statistical, frequency, fractal, and chaos analyses) to laser Doppler anemometry (LDA) data for flow regime identification in bubble columns.

It is noteworthy that even minute traces of contaminants in the tap water can change the transition between flow regimes [23]. Furthermore, it has been reported that porous spargers with mean pore sizes of less than 150 μm generally produce bubbly flows up to U_G values of about 0.05–0.08 m s^{-1}, while for perforated plates with orifice diameters larger than 1×10^{-3} m, bubbly flow may not occur in case of pure liquids.

In some works [7, 17] only the first transition velocity was identified, while in other papers the identification criterion was unclear. For instance, Lin et al. [8] used a local maximum in some cases, whereas in other cases they used a local minimum. The information entropy theory [17] is also not very sensitive to every flow regime transition. Thus, new powerful and reliable methods should be developed that are able to precisely identify the two main transition velocities.

Table 1. Overview of the different methods applied for flow regime identification in bubble columns.

Literature source	Applied method	Measured signal
Lockett and Kirkpatrick [6]	drift-flux analysis	pressure fluctuations
Letzel et al. [7]	nonlinear chaos analysis	absolute pressure
Lin et al. [8]	nonlinear chaos analysis	differential pressure
Ajbar et al. [9]	nonlinear chaos analysis	acoustic time series
Nedeltchev et al. [10]	nonlinear chaos analysis	particle trajectories
Nedeltchev et al. [11]	nonlinear chaos analysis	photon counts
Nedeltchev et al. [12]	nonlinear chaos analysis	differential pressure
Kikuchi et al. [13]	nonlinear chaos analysis	bubble frequency
Drahoš et al. [14]	Hurst analysis	pressure time series
Vial et al. [15], Gourich et al. [16]	statistical analysis	pressure fluctuations
Letzel et al. [7], Ajbar et al. [9]	spectral analysis	pressure fluctuations
Nedeltchev and Shaikh [17]	information entropy theory	photon counts

2 The Essence of the New Method

Nedeltchev et al. [24] found that, when the range of the gas holdup time series signal was divided into different regions (with progressively increasing heights proportional to the division step of 0.25, i.e. 1×0.25, 2×0.25, 3×0.25, 4×0.25, etc., shown in Fig. 1a), the maximum number of signal visits N_v^{max} (step 0.25) (see the grey box in Fig. 1 a) in one of these regions was capable of identifying the two main transition velocities U_{trans} in the bubble column operation. The only disadvantage of this approach is that the N_v^{max} (step 0.25) values depended on the division scheme, i.e., the selection of the division step.

In order to eliminate this dependence on the selection of the division scheme, the range of each signal was divided in two different ways (with steps of 0.25 and 0.5), which accordingly yielded two different N_v^{max} values. At first, both the minimum and maximum values of the gas holdup signal (measured as percentage) were determined and then the signal range was divided into different regions (with progressively increasing heights) by using the division step of 0.25 as explained above (Fig. 1 a). The most frequently visited region (marked by a grey box) is indicated as N_v^{max} (step 0.25). Secondly, the same signal range was divided into different regions by means of step 0.5 (with progressively increasing heights: 1×0.5, 2×0.5, 3×0.5, 4×0.5, etc.; shown in Fig. 1 b). When a bigger division step is used, the maximum number of visits in a region N_v^{max} increases. In addition, the division scheme with a smaller step is characterized by more regions. In the second division pattern, the most frequently visited region is indicated as N_v^{max} (step 0.5). The new dimensionless parameter N_r^{max} (also called "relative maximum number of visits in a region") is a function of both step-dependent N_v^{max} values:

$$N_r^{max}(1) = \frac{N_v^{max}(\text{step } 0.5) - N_v^{max}(\text{step } 0.25)}{(0.5 - 0.25)} \quad (1)$$

In this form, the new dimensionless parameter N_r^{max} is step independent and it can be used as a powerful tool for flow regime identification.

In order to demonstrate that it is really a step-independent parameter, the N_v^{max} values were also calculated at two different steps: 0.5 and 0.1. In this case, Eq. (1) was redefined as follows:

$$N_r^{max}(2) = \frac{N_v^{max}(\text{step } 0.5) - N_v^{max}(\text{step } 0.1)}{(0.5 - 0.1)} \quad (2)$$

The transition velocities U_{trans} identified by means of N_r^{max} (1) and N_r^{max} (2) will be compared and it will be shown that the new index does not depend on the preselection of any other parameter. It is worth noting that, when the division step becomes too small (for instance, equal to 0.1), counting of the number of visits in each region becomes very complicated since there are many values lying on the boundaries between two different regions. So, in principle, the division step should not be too small.

3 Experimental Setup

The small bubble column had an inner diameter (i.d.) of 0.15 m and was equipped with a perforated plate distributor (14 holes, Ø 4×10^{-3} m, open area (OA) = 1 %). The large bubble column had an i.d. of 0.4 m and was equipped with a similar type of perforated plate distributor (101 holes, Ø 4×10^{-3} m, OA = 1 %). Both bubble columns were operated with an air/deionized water system under ambient conditions. The clear liquid height in both columns was adjusted at 2.0 m.

The time series (60 000 points) of the cross-sectional averaged gas holdup (recorded as percentage) in both bubble columns were measured by means of conductivity wire-mesh sensors (Fig. 2).

Figure 2. Photograph of the applied wire-mesh sensor with an i.d. of 0.15 m.

The wire-mesh sensors consisted of two electrode planes each with 24 (in the case of the small column) or 64 (in the case of the large column) stainless-steel wires of 0.2×10^{-3} m and 6.125×10^{-3} m distance between the wires. The distance between the planes was 4.0×10^{-3} m and the wires from differ-

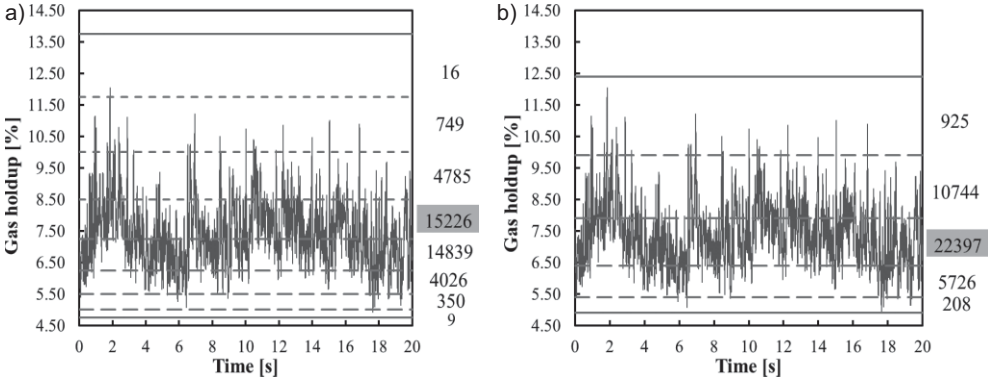

Figure 1. Example of the cross-sectional averaged gas holdup time series data (40 000 points, 20 s) obtained by the wire-mesh sensor (f_s = 2000 Hz) in the large bubble column (D_c = 0.40 m) for a step size equal to (a) 0.25 , (b) 0.5, at U_G = 0.023 m s^{-1}.

ent planes crossed each other at right angles. This arrangement gave 576 (in the small column) or 4096 (in the large column) crossing points, 78 % thereof inside the circular cross-section of the columns. One plane of the electrodes acted as a transmitter, the other one as a receiver. The transmitter electrodes were activated by a multiplexing circuit in successive order, and signals derived from the current measured at the receiver electrodes were stored. After one multiplexing cycle, a two-dimensional matrix of values was available, reflecting the conductivities between all crossing points of the electrodes of the two perpendicular planes. The signals of the matrix were converted into gas holdup data based on proper calibration measurements on the liquid-flooded and empty column, respectively. The wire-mesh sensor technology is described in more detail by Prasser et al. [25]. The wire-mesh sensor was always installed at 1.3 m above the gas distributor.

In the case of organic liquids (with very low electrical conductivity), a capacitance wire-mesh sensor can be used. Such a capacitance wire-mesh sensor has already been designed and manufactured at our institute. Our conductivity and capacitance wire-mesh sensors have a simple design and they can be fitted into any industrial bubble column. The sensors can be built in many different design types.

4 Results and Discussion

In the narrow (0.15 m i.d.) bubble column, two well-pronounced local minima (Fig. 3) in the profiles of the new parameters, N_r^{max} (1) and N_r^{max} (2), were identified. At $U_G = 0.034\ m\ s^{-1}$, the end of the gas maldistribution regime was observed. This regime existed due to the relatively large size ($Ø\ 4 \times 10^{-3}$ m) of the hole openings. The first U_{trans} value is very close to the one calculated theoretically ($0.029\ m\ s^{-1}$) by the correlation of Reilly et al. [26]. The physical meaning of the first transition velocity is to show at which superficial gas velocity U_G the gas maldistribution regime discontinues. The onset of the churn-turbulent flow regime was identified (based on a local minimum) at $U_G = 0.089\ m\ s^{-1}$. The second transition velocity indicates the onset of bubble coalescence (the formation of many spherical-cap bubbles in the core). It is worth noting that in the transition flow regime both profiles exhibited a monotonous declining trend.

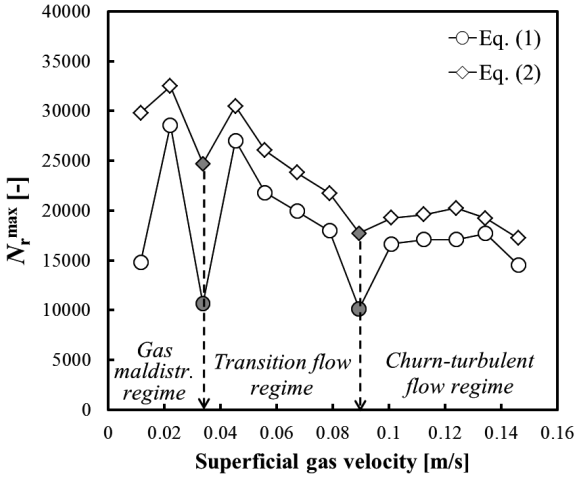

Figure 3. N_r^{max} (1) and N_r^{max} (2) values as a function of U_G in the small column.

The results in Fig. 3 show that the new parameter N_r^{max} is not very sensitive to the scheme of division (provided that the difference between the two division steps is not smaller than 0.25). The two local minima in N_r^{max} (1) and N_r^{max} (2) occurred at the same U_G values. However, the local minima were more pronounced at the smaller step difference (0.5–0.25; see Eq. 1).

The well-pronounced local minima of the new parameter N_r^{max} exhibit that the signal is better (or more equally) distributed between its minimum and maximum values at these critical U_G values, and that is why the N_r^{max} values are the lowest. In other words, the degree of order of the signal improves at each transition velocity U_{trans}.

It is very important to mention that the two U_{trans} values identified in Fig. 3 can also be identified based on the N_v^{max} (step 0.5) profile (Fig. 4 a). The same identification criterion (local minimum) was used. In addition, the maximum information entropies IE_{max} were estimated on the basis of this data. The algorithm described in [17] was used. The only difference was that, in the estimation of the probability, the height of the largest region multiplied by 60 000 visits was used in the denominator. Fig. 3 b shows two local minima occurring at 0.034 and 0.089 m s^{-1}, and they are in full agreement with both the N_r^{max} and N_v^{max} (step 0.5) results.

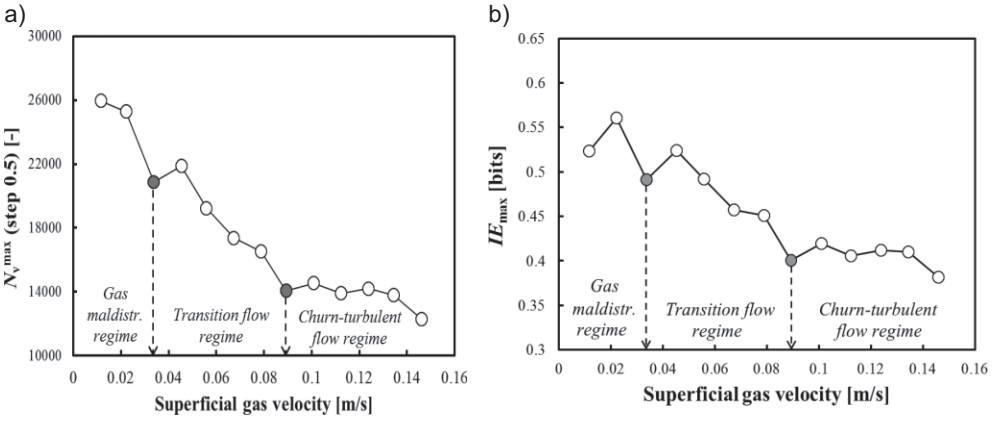

Figure 4. Profiles of (a) N_v^{max} (step 0.5) and (b) IE_{max} as a function of U_G in the large bubble column.

It is noteworthy that such two well-pronounced local minima cannot be identified in the profiles of many other parameters derived on the basis of different theories (Kolmogorov entropy [7], metric entropy [8], largest Lyapounov exponent [8], correlation dimension [8], mutual information [8], maximum information entropy [17], average absolute deviation, mean, etc.). Usually, the researchers mix the identification criteria and sometimes use the local minimum and sometimes the local maximum for the sake of flow regime identification.

In order to illustrate the existence of the gas maldistribution regime, several photographs were taken at different U_G values in the vicinity of the gas sparger, as shown in Fig. 5. The photographs show that bubbles were formed at all distributor openings for the first time at $U_G = 0.04\,m\,s^{-1}$ (case d). At lower U_G values (cases a–c), a clear gas maldistribution was observed. So, the new parameter N_r^{max} can correctly identify the end of the gas maldistribution regime.

Fig. 6 shows that the new parameter N_r^{max} can also identify the two U_{trans} values in the large bubble column (0.4 m i.d.). The first U_{trans} value is distinguishable (based on the well-pronounced local minimum) at $U_G = 0.034\,m\,s^{-1}$. Both the profiles of N_r^{max} (1) and N_r^{max}(2) exhibited a well-pronounced minimum at this critical velocity. A comparison between the results given in Figs. 3 and 6 reveals that the column diameter D_c does not have an effect on the first U_{trans} value, which is in agreement with the empirical formulas available in the literature [26, 27].

The second U_{trans} value was identified at $U_G = 0.078\,m\,s^{-1}$ (see the second local minimum in both the N_r^{max}(1) and N_r^{max}(2) profiles in Fig. 6). This result means that the increase in D_c shifts the onset of the churn-turbulent flow regime to somewhat lower U_G values, and thus, the transition regime becomes slightly narrower.

Fig. 7 a shows that the N_v^{max} (step 0.5) profile in the large column yields identical U_{trans} values to the ones identified in Fig. 6. Two well-pronounced local minima were observed at $U_G = 0.034$ and $0.078\,m\,s^{-1}$. The comparisons between Figs. 3 and 4 and Figs. 5 and 6 imply that the correct division step (yielding the correct U_{trans} values) is equal to 0.5. This conclusion can be reached only with the help of the new parameter N_r^{max}. Based on the N_v^{max} (step 0.5) data, the maximum information entropies IE_{max} [17] were calculated. Fig. 7 b shows that two well-pronounced local minima identified the same U_{trans} values (0.034 and $0.078\,m\,s^{-1}$).

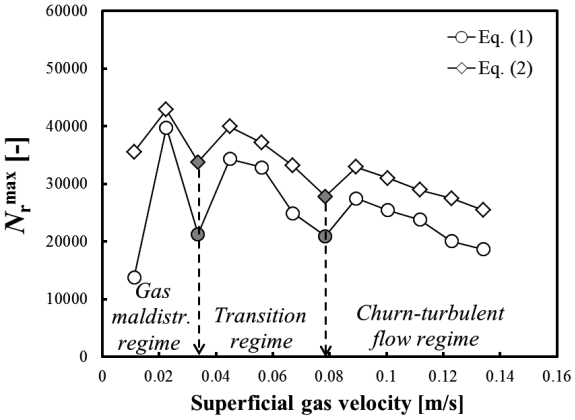

Figure 6. N_r^{max}(1) and N_r^{max}(2) values as a function of U_G in the large bubble column.

Fig. 8 shows several photographs of the bubble formation process in the vicinity of the gas sparger at different U_G values. It is obvious that gas maldistribution prevailed up to $U_G = 0.03\,m\,s^{-1}$, and above this critical value, bubble formation from all distributor holes was observed. Therefore, the results shown in Figs. 6 and 7 for the first U_{trans} value are in agreement with the flow visualization in the large bubble column.

The results regarding the transition velocities identified in both columns are summarized in Tab. 2. As was mentioned above, the column diameter D_c has an effect only on the second U_{trans} value.

Nedeltchev et al. [24] identified the two transition velocities U_{trans} (0.022 and $0.112\,m\,s^{-1}$) in the narrow column on the basis of the local minima in both the Kolmogorov entropy and the N_v^{max} (step 0.25) profiles. The photographs in Fig. 5 prove that both parameters identify the first U_{trans} value somewhat earlier than the real case. Nedeltchev and Schubert [28] introduced another parameter (average/(3 × (average absolute deviation)), which precisely identified the first U_{trans} value ($0.034\,m\,s^{-1}$) in the narrow bubble column. However, in the bigger column, the new parameter identified the first U_{trans} value at a somewhat higher value ($0.045\,m\,s^{-1}$). So, the new parameter (N_r^{max}(1) or N_r^{max}(2)) defined in this article is the most reliable and precise one.

In summary, the main findings are the values of the two main transition velocities in both the small and the large bubble column. Both transition velocities are important design parameters for bubble columns. On the basis of a new and original parameter, it is shown that the column diameter affects only the second critical velocity. The paper shows that perforated plates

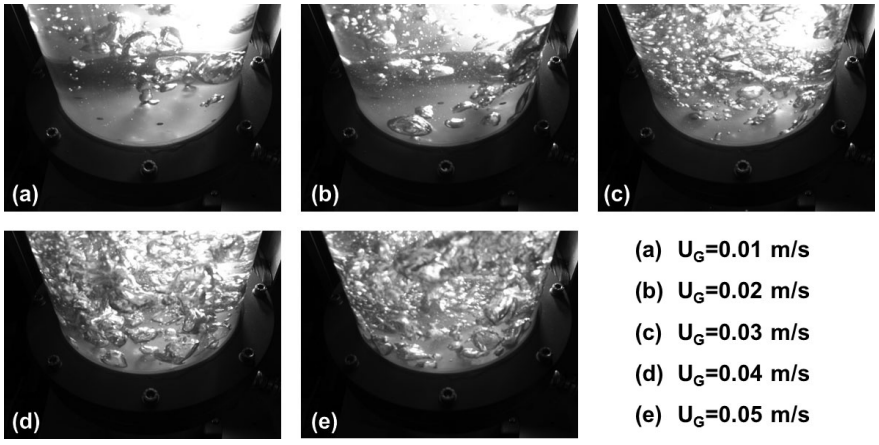

Figure 5. Visualization of the gas maldistribution regime in the small bubble column.

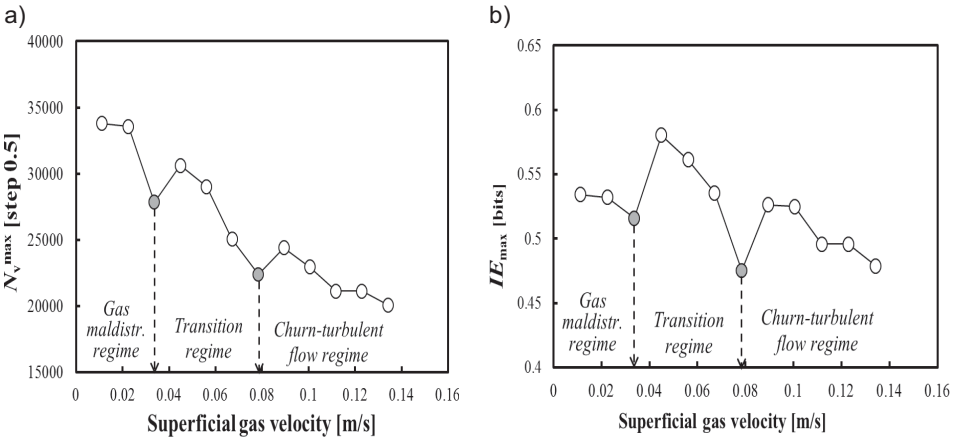

Figure 7. Profiles of (a) N_v^{max} (step 0.5) and (b) IE_{max} as a function of U_G in the large bubble column.

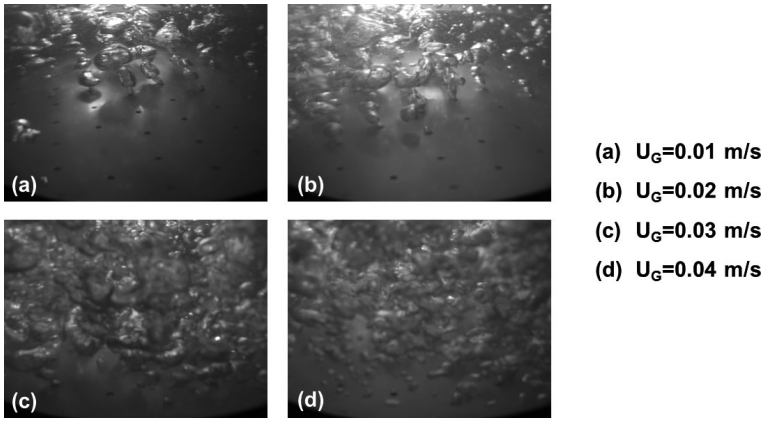

Figure 8. Visualization of the gas maldistribution regime in the large bubble column.

Table 2. Summary of the transition velocities identified in both bubble columns.

Identification method	D_c [m]	First U_{trans} [m s^{-1}]	Second U_{trans} [m s^{-1}]
$N_r^{max}(1)$	0.15	0.034	0.089
$N_r^{max}(2)$	0.15	0.034	0.089
N_v^{max} (step 0.5)	0.15	0.034	0.089
IE_{max}	0.15	0.034	0.089
$N_r^{max}(1)$	0.4	0.034	0.078
$N_r^{max}(2)$	0.4	0.034	0.078
N_v^{max} (step 0.5)	0.4	0.034	0.078
IE_{max}	0.4	0.034	0.078

with hole openings of 4×10^{-3} m generate a gas maldistribution regime, so the hole openings should be (much) smaller than 4×10^{-3} m. By means of the new parameter, the boundaries of the gas maldistribution regime can be identified.

It is noteworthy that the new method relies on experimental data and that the results are not directly applicable to a different industrial column equipped with a different gas distributor and/or operated with an organic liquid. For this purpose, new measurements should be performed and further analyzed by means of the new parameter.

5 Conclusions

A new dimensionless statistical parameter, N_r^{max}, was defined on the basis of the division of the signal range into different regions by means of different steps. In the small bubble column (0.15 m i.d.), two local minima in the N_r^{max} profile were observed at U_G = 0.034 and 0.089 m s^{-1}. They identified the two main transition velocities U_{trans}. In the large column (0.4 m i.d.), the N_r^{max} profile exhibited two local minima at U_G = 0.034 and 0.078 m s^{-1}. As the column diameter increased, the first U_{trans} remained the same, whereas the second U_{trans} decreased to some extent. For both bubble columns, the effect of the division scheme on the N_r^{max} profiles was found to be insignificant. The results were supported by photographs taken in both columns.

On the basis of the profiles of the new statistical parameter N_r^{max} in both columns, it was determined that, when the signal was divided into different regions with a step of 0.5, both U_{trans} values were accurately identified. The maximum information entropies extracted from this data can also be used for flow regime identification.

In the case of the small column, a comparison among the U_{trans} values identified by the new parameter N_r^{max}, the Kolmogorov entropy, and another statistical parameter was performed. It was found that only the transition velocities identified by the new parameter N_r^{max} were in agreement with the flow visualization images in both columns.

Acknowledgment

S.N. is grateful to the European Commission for providing him with a Marie Curie Outgoing International Fellowship (7th Framework Programme, Grant Agreement No. 221832, 2010–2013). M.S. gratefully acknowledges the financial support of the European Research Council (ERC Starting Grant, Grant Agreement No. 307360). The financial support of the Helmholtz Association of German Research Centers within the frame of the Initiative and Networking Fund is also acknowledged (No. ERC-0010).

The authors have declared no conflict of interest.

Symbols used

D_c	[–]	column diameter
f_s	[Hz]	sampling frequency
IE_{max}	[bits]	maximum information entropy
N_v^{max}	[–]	maximum number of visits in a single region
N_r^{max}	[–]	relative maximum number of visits in a region
$N_r^{max}(1)$	[–]	relative maximum number of visits in a region at steps 0.5 and 0.25, Eq. (1)
$N_r^{max}(2)$	[–]	relative maximum number of visits in a region at steps 0.5 and 0.10, Eq. (2)
N_v^{max} (step 0.5)	[–]	maximum number of visits in a region at step 0.5
N_v^{max} (step 0.25)	[–]	maximum number of visits in a region at step 0.25
N_v^{max} (step 0.1)	[–]	maximum number of visits in a region at step 0.1
U_G	[m s^{-1}]	superficial gas velocity
U_{trans}	[m s^{-1}]	transition gas velocity

References

[1] Y. T. Shah, B. G. Kelkar, S. P. Godbole, W.-D. Deckwer, *AIChE J.* **1982**, *28 (3)*, 353–379. DOI: 10.1002/aic.690280302
[2] J. Ellenberger, R. Krishna, *Chem. Eng. Sci.* **1994**, *49 (24)*, 5391–5411. DOI: 10.1016/0009-2509(94)00274-6
[3] J. H. Hills, R. C. Darton, *Trans. Inst. Chem. Eng.* **1976**, *54*, 258–264.
[4] H. F. Bach, T. Pilhofer, *Ger. Chem. Eng.* **1978**, *1 (5)*, 270–275.
[5] K. Franz, T. Börner, H. J. Kantorek, R. Buchholz, *Ger. Chem. Eng.* **1984**, *7*, 365–374.
[6] M. J. Lockett, R. D. Kirkpatrick, *Trans. Inst. Chem. Eng.* **1975**, *53*, 267–273.
[7] H. M. Letzel, J. C. Schouten, R. Krishna, C. M. Van den Bleek, *Chem. Eng. Sci.* **1997**, *52 (24)*, 4447–4459. DOI: 10.1016/S0009-2509(97)00290-X
[8] T.-J. Lin, R.-C. Juang, Y. C. Chen, C.-C. Chen, *Chem. Eng. Sci.* **2001**, *56 (3)*, 1057–1065. DOI: 10.1016/S0009-2509(00)00322-5
[9] A. Ajbar, W. Al-Masry, E. Ali, *Chem. Eng. Proc.* **2009**, *48 (1)*, 101–110. DOI: 10.1016/j.cep.2008.02.004
[10] S. Nedeltchev, S. B. Kumar, M. P. Duduković, *Can. J. Chem. Eng.* **2003**, *81 (3/4)*, 367–374. DOI: 10.1002/cjce.5450810305
[11] S. Nedeltchev, A. Shaikh, M. Al-Dahhan, *Chem. Eng. Technol.* **2006**, *29 (9)*, 1054–1060. DOI: 10.1002/ceat.200600162
[12] S. Nedeltchev, U. Jordan, O. Lorenz, A. Schumpe, *Chem. Eng. Technol.* **2007**, *30 (4)*, 534–539. DOI: 10.1002/ceat.200600344
[13] R. Kikuchi, T. Yano, A. Tsutsumi, K. Yoshida, M. Puncochar, J. Drahoš, *Chem. Eng. Sci.* **1997**, *52 (21/22)*, 3741–3745. DOI: 10.1016/S0009-2509(97)00220-0
[14] J. Drahoš, F. Bradka, M. Puncochar, *Chem. Eng. Sci.* **1992**, *47 (15/16)*, 4069–4075. DOI: 10.1016/0009-2509(92)85158-8
[15] C. Vial, E. Camarasa, S. Poncin, G. Wild, N. Midoux, J. Bouillard, *Chem. Eng. Sci.* **2000**, *55 (15)*, 2957–2973. DOI: 10.1016/S0009-2509(99)00551-5
[16] B. Gourich, C. Vial, A. Essadki, F. Allam, M. B. Soulami, M. Ziyad, *Chem. Eng. Proc.* **2006**, *45 (3)*, 214–223. DOI: 10.1016/j.cep.2005.09.002
[17] S. Nedeltchev, A. Shaikh, *Chem. Eng. Sci.* **2013**, *100*, 2–14. DOI: 10.1016/j.ces.2013.03.039
[18] M. R. Bhole, J. B. Joshi, *Chem. Eng. Sci.* **2005**, *60 (16)*, 4493–4507. DOI: 10.1016/j.ces.2005.01.004
[19] E. Olmos, C. Gentric, N. Midoux, *Chem. Eng. Sci.* **2003**, *58 (10)*, 2113–2121. DOI: 10.1016/S0009-2509(03)-00013-7
[20] S. M. Monahan, V. S. Vitankar, R. O. Fox, *AIChE J.* **2005**, *51 (7)*, 1897–1923. DOI: 10.1002/aic.10425
[21] M. Simmonet, C. Gentric, E. Olmos, N. Midoux, *Chem. Eng. Proc.* **2008**, *47 (9/10)*, 1726–1737. DOI: 10.1016/j.cep.2007.08.015
[22] E. Olmos, C. Gentric, S. Poncin, N. Midoux, *Chem. Eng. Sci.* **2003**, *58 (9)*, 1731–1742. DOI: 10.1016/S0009-2509(03)00002-2
[23] J. L. Anderson, J. A. Quinn, *Chem. Eng. Sci.* **1970**, *25 (3)*, 373–380. DOI: 10.1016/0009-2509(70)80036-7
[24] S. Nedeltchev, T. Donath, S. Rabha, U. Hampel, M. Schubert, *J. Chem. Eng. Jpn.* **2014**, *47 (9)*, 722–729. DOI: 10.1252/jcej.13we362
[25] H.-M. Prasser, A. Böttger, J. Zschau, *Flow Meas. Instrum.* **1998**, *9 (2)*, 111–119. DOI: 10.1016/S0955-5986(98)00015-6
[26] I. G. Reilly, D. S. Scott, T. De Bruijn, D. MacIntyre, *Can. J. Chem. Eng.* **1994**, *72 (1)*, 3–12. DOI: 10.1002/cjce.5450720102
[27] P. M. Wilkinson, A. P. Spek, L. L. Van Dierendonck, *AIChE J.* **1992**, *38 (4)*, 544–554. DOI: 10.1002/aic.690380408
[28] S. Nedeltchev, M. Schubert, *J. Chem. Eng. Jpn.* **2015**, *48 (2)*, 107–111. DOI: 10.1252/jcej.14we189

